Available online at www.sciencedirect.com

ScienceDirect

Procedia CIRP 144 (2026) 210–215

www.elsevier.com/locate/procedia

8th CIRP Conference on Surface Integrity

Evaluation of the achievable surface topographies, dimensional and geometrical tolerances in hybrid manufacturing of PLA parts by Fused Filament Fabrication (FFF) and milling

Laurent Spitaels[a]*, Valentin Dambly[a], Margaux Lorenzoni[a], Gregory Martic[b], Cathy Delmotte[b], Enrique Juste[b], Édouard Rivière-Lorphèvre[a], Fabrice Petit[b] and François Ducobu[a]

[a]*UMONS Research Institute for Materials Science and Engineering, University of Mons, Place du Parc 20, 7000 Mons, Belgium*

[b]*Belgium Ceramic Research Centre (BCRC), Avenue Gouverneur Cornez 4, 7000 Mons, Belgium*

* Corresponding author. *E-mail address:* laurent.spitaels@umons.ac.be

Abstract

Hybrid manufacturing combining additive and subtractive processes is a promising approach for overcoming the inherent staircase effect and the low dimensional and (micro-)geometrical accuracy of 3D printers. Furthermore, finishing the part directly within the same machine prevents positioning errors and decreases the risk of generating scrap. Nevertheless, despite a significant research interest in hybrid machines, their capability in terms of surface topography and tolerances have not been fully evaluated. Therefore, this paper aims to quantify the benefits of manufacturing PLA parts using a hybrid approach that combines Fused Filament Fabrication (FFF) and milling. The finishing operation removed the staircase effect from the part, generating flat, homogeneous surface topography. The arithmetic roughness (Ra) decreased by two classes (from Ra 12.5 µm to Ra 3.2 µm), while the areal equivalent (Sa) was reduced from 20 µm to 6 µm. Total Roughness (Rt) and Maximum Height (Sz) showed a similar trend, with reductions up to 85%, Rt below 30 µm and Sz below 200 µm were obtained. There was a slight improvement in dimensional tolerance for the dimensions across the printer Z-axis (from IT14 to IT11 according to ISO 286-1:2010). However, larger tolerances (from IT14 to IT15) were obtained for those across the X and Y axes. The parallelism, perpendicularity and flatness of the parts were significantly improved, leading to an H (fine) class for almost all surfaces according to ISO 2768-2:1989. This demonstrates the benefits of the hybrid approach.

Peer-review under responsibility of the scientific committee of the Scientific committee of the CIRP CSI 2026

Keywords: Hybrid Manufacturing; Material Extrusion; Milling; Surface topography; Tolerances; PLA.

1. Introduction

Additive Manufacturing (AM) and, especially, Material Extrusion (MEX) promises to reduce the manufacturing costs for producing small or unique series of parts in advanced materials such as metallic alloys and technical ceramics [1,2]. This could be achieved by using already mature feedstock such as pellets initially dedicated to injection molding, melting them and depositing layers using the Fused Granular Fabrication process (FGF), one derivative of MEX [3]. Nevertheless, the current capability of MEX in terms of surface topographies [4], dimensional and geometrical tolerances still hampers its widespread and limits it to prototyping or non-demanding applications [5,6]. One solution can be to finish the produced parts using a process capable of meeting very tight tolerances and surface topographies, such as milling [7]. However, switching from one machine to another can generate parts positioning error,

Peer-review under responsibility of the scientific committee of the Scientific committee of the CIRP CSI 2026
10.1016/j.procir.2026.02.075

especially if the part design is freeform with complex rough surfaces, difficult to probe using standard devices. Moreover, the contact needed between the milling tool and the part during the finishing process limits the designs that can be finished, while AM is usually chosen to enable the generation of complex design (internal cavities or lattices for example). These features are impossible to finish with a milling tool if the part is already printed due to a lack of accessibility [8].

These limitations motivate the development of hybrid machines combining the additive and subtractive processes within the same volume [7,9]. Printing with AM can be stopped after a few layers to allow the milling tool to finish the surfaces while they are still accessible. These steps can then be repeated until the final desired design is obtained. A significant effort was made to develop hybrid machines printing directly metallic parts using, for example, Directed Energy Deposition (DED) and milling, with commercial machines already available for a decade [10]. However, their cost is still very high, limiting their use to large companies that can afford them. The development of more affordable hybrid machines, relying on an indirect process such as FGF for metallic and ceramic materials, is then of prime interest [11]. Nevertheless, these machines are still at an early development stage with limited knowledge of the surface topographies, dimensional and geometrical tolerances that can be achieved. Indeed, the current research has not addressed the achievable tolerances, while the surface topography evaluation is usually limited to profile parameters [12–14]. Despite the potential of FGF, Fused Filament Fabrication (FFF) was selected for this study. Indeed, affordable FGF printers are not yet widespread, while most of them are the result of modifying an FFF printer. This is the path that will be followed in the future. Combining FFF and milling is then a first step toward obtaining a hybrid machine with FGF.

Therefore, this paper proposes evaluating the performance of a hybrid machine constructed from an E3D ToolChanger fitted with a FFF extruder and a spindle. The surface topography, dimensional and geometrical tolerances of parts are evaluated before and after milling, with all operations being performed in the same machine.

2. Method

2.1. Hybrid machine

The machine considered for shaping the parts by AM and finishing them using milling is shown in Figure 1. It consists of an E3D ToolChanger that was modified with the addition of a Genmitsu spindle (GS-775M). This printer was already capable of selecting different FFF extruders using its embedded tool picker. The added spindle is a DC current motor able to deliver 75 W, can reach a maximum of 20,000 rpm and can be fitted with milling tools of various diameters (from 1 mm to 7 mm) using an ER11 collet. The spindle was installed in the machine using a milled adaptation part made of 6082 Aluminum Alloy and mounted on a dedicated additional HIWIN carriage to improve the rigidity. This configuration, shown in Figure 2, was chosen to avoid generating detrimental vibrations when milling parts, as experienced by other research teams [12]. The available building/milling area was then reduced from 363 mm x 265 mm to 281 mm x 225 mm according to the X and Y axes of the machine. The control of the spindle speed is ensured by the DUET2 board of the ToolChanger, while a Pololu motor drive as well as a dedicated additional power supply were used to drive the spindle.

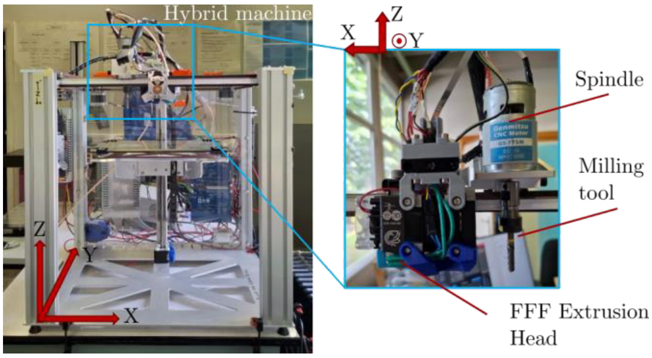

Figure 1 Hybrid machine and its FFF extruder and spindle.

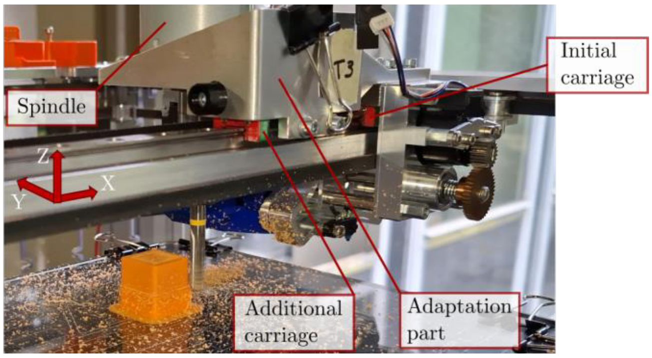

Figure 2 Adaptation part and additional carriage for the spindle.

2.2. Overall experimental steps and parts manufacturing

To evaluate the achievable surface topographies, and the dimensional and geometrical tolerances, a simple part design was chosen as depicted in Figure 3. It consists of a cube with 20 mm edges. 2 mm radius fillets were also added on the vertical edges to reduce the risk of warping as advised by Pei et al. [15] for the FFF process. This is then the desired geometry that should be obtained by FFF or by combining FFF and milling (hybrid). The parts were modelled using SolidWorks 2024, while their geometry was exported in .STL using the finest available resolution of the Software.

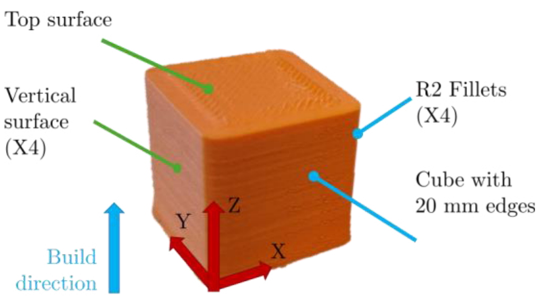

Figure 3 Part design manufactured by FFF.

Two main steps were followed as depicted in Figure 4:

- The first consists in producing the desired design three times exclusively by AM to evaluate the achievable surface topographies as well as dimensional and geometrical tolerances for the AM process alone. This also allowed to determine the thickness to be removed by the milling operation, as well as the machining allowance.
- The second step is the production by AM of three other parts followed by their finishing by milling operations within the same machine. Each of the parts is completely produced by AM and then finished. This is the first step before future full hybrid operations alternating additive and subtractive processes together. The selected parameters and operating conditions for both processes are detailed in the following sections as well as the characterizations that were conducted on the parts. Since the parts are milled, their dimensions are those presented in Figure 3 to which machining allowances have been added. These are presented in Section 2.5.

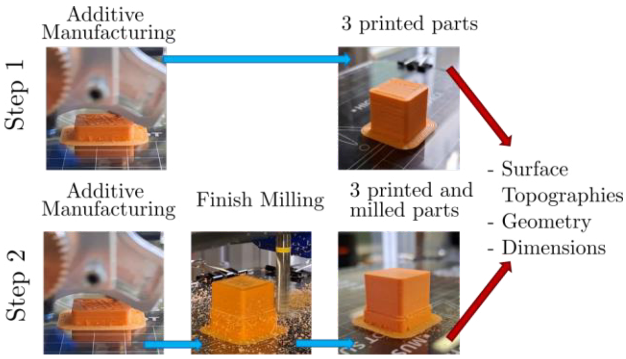

Figure 4 Steps followed during the experiments.

2.3. Part characterizations

The parts were characterized using two main devices: a Coordinate Measuring Machine Wenzel LH54 and a Keyence VR6000 profilometer.

The first was used to determine the dimensions (distances between the vertical faces and total height) and geometry (flatness, perpendicularity and parallelism of the faces) of the parts. The CMM exhibits a measurement uncertainty of 3 µm + L/300 for the X and Y axes and 3.5 µm + L/300 for the Z-axis, L in mm. Each of the parts face was evaluated with 12 points randomly distributed. The selected spherical ruby probe exhibited a diameter of 5 mm and was supplied by Renishaw. This allowed filtering the staircase effect generated by FFF. For consistency, the same configuration was used for the as-built and milled parts.

The profilometer was used to evaluate the surface topographies. It exhibited a measurement accuracy of ± 2 µm for the X and Y axes and ± 4 µm for Z-axis. The chosen indicators were Ra, Rt, Sa and Sz. The first two were evaluated by taking 10 different lines of 12 mm on each surface, while the areal parameters were determined using surfaces of 15 mm by 12 mm. The low-pass filter cut-off selected for Ra and Rt was 0.8 mm, while the areal parameters were evaluated using a 2.5 mm cut-off, following ISO 21920:2021 and ISO 25178-2:2021, respectively.

2.4. Printing

The parts were all printed using a FFF E3D Hemera extruder. A Polymaker PolyTerra PLA filament of 1.75 mm of diameter was the selected feedstock. The slicing was performed using PrusaSlicer version 2.9.2 with the printing parameters given in Table 1. To ensure better adhesion of the part, a light mist of 3DLAC was sprayed on the glass build platform, while a brim of 5 mm was added to the part design. The parts walls and top surface thicknesses were chosen in accordance with the machining allowances that were determined. This choice ensured sufficient part stiffness during the finish milling, while allowing a 50% porous core, saving material (Figure 5).

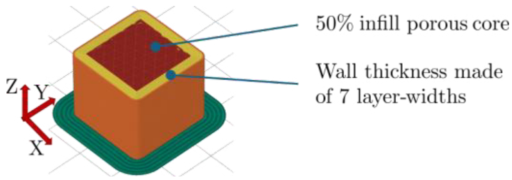

Figure 5 Cut view of the parts walls (yellow and orange) and core (red).

Table 1 Printing parameters for the manufacturing of the parts using FFF.

Nozzle diameter	0.4 mm
Layer thickness (first layer)	0.15 mm (0.2 mm)
Nozzle & build platform temperatures	205°C & 60°C
Infill strategy and density	Cubic, 50%
Wall thickness	7 layer-widths
Top & bottom thickness	14 & 2 layer-heights
Printing time	~ 35 min

2.5. Determination of the required machining allowances

Prior to conducting the finishing operations, the machining allowances must be determined. Indeed, producing a part by AM with dimensions slightly larger than those required will ensure that there is sufficient material on each of its surfaces to be removed. This determination was made by measuring the 3 first produced parts and comparing their surface topography, dimensions and geometry with those desired. For consistency, these preliminary measurements were conducted using the conditions described in Section 2.3.

Since the milling operation should correct the surface topography as well as the geometry, the machining allowances were chosen as the sum of the Maximum Height (Sz) and the form error (parallelism between the top surface and build platform and perpendicularity between the build platform and the vertical surfaces). For the form error, a conservative choice was made by selecting the maximum between parallelism and perpendicularity deviation. These measurements are presented in Table 2.

For the vertical surfaces, the obtained machining allowance is 0.589 mm, while it reaches 1.325 mm for the top surface. These dimensions must be added to the CAD model to obtain the stock, while considering the constraints of the AM process. Indeed, the height and width of the part should be integers that are multiples of the layer height and layer width, respectively. This then led to a part height of 21.330 mm (141 layers of 0.15 mm + the first layer thickness of 0.2 mm) and a part width of 21.200 mm (53 widths of 0.4 mm). This means that 0.6 mm should be removed from the parts sides and 1.330 mm on its top surface to obtain the desired cube with 20 mm edges long. This already demonstrates a lower quality for the generation of the top surface compared to the vertical ones. This difference in quality could be due to a slight over-extrusion during the printing process.

Table 2 Maximal surface topographies and form deviations achieved.

Surface	Max Sz [µm]	Max form deviation [mm]
Vertical	402	0.187 of Perpendicularity
Top	882	0.443 of Parallelism

2.6. Finish milling

The finishing of the parts was performed directly on the build platform, while keeping it at the temperature selected for the printing (60°C). This ensured the parts adhesion to the build platform. The selected milling tool was a solid end-mill with a cylindrical shape, a diameter of 6 mm and three teeth supplied by Hoffmann (reference Garant 209425-6).

Two main milling operations were conducted: contouring the vertical faces of the parts and surfacing their top surface. The main cutting parameters are given in Table 3. The cutting speed and feed rate were chosen accordingly to a previous study [16]. All the milling operations were conducted using down milling, while the gcode was generated using RhinoCAM 14 and Rhinoceros 8. First, the contouring operations were performed on the parts vertical walls, followed by the surfacing of the top surface. A safety margin of 5 mm above the build platform was kept in Z, leading to 5 mm of the parts remaining uncut (as shown in Figure 6).

Table 3 Cutting parameters for the finish milling of the parts.

Cutting speed (v_c) & spindle speed (N)	75.4 m/min & 4000 rpm
Feed rate (v_f)	800 mm/min
Contouring depths of cut	Radial (a_e): 0.1 mm
	Axial (a_p): 0.5 mm
Surfacing depths of cut	Radial (a_e): 0.5 mm
	Axial (a_p): 0.1 mm
Finish milling time	~ 65 min

3. Results and discussion

3.1. Qualitative evaluation

Figure 6 gives a qualitative overview of the as-built as well as the milled parts. As it can be seen, the as-built parts exhibit AM typical defects such as staircase effect on the vertical surfaces as well as a poor surface topography for the connection between the walls and the infill in the top surface. These defects were corrected with the finish milling operations, leading to smoother and more homogeneous surface topographies, both on the vertical and top surfaces. As presented previously, 5 mm remained uncut on each finished part vertical surface (safety margin for the milling).

3.2. Surface topography evaluation

Figure 7 presents the results of Arithmetic Roughness (Ra) and Arithmetic Mean Height (Sa) for the as-built and milled parts. Each bar in the graph represents the average values collected over three parts, given with ±σ error bars. A distinction is made between the top (Z) and vertical (XY) surfaces. The graphs in the following sections are constructed using a similar approach.

The finish milling operation allowed to decrease Ra from two classes (from Ra 12.5 µm to Ra 3.2 µm). Sa followed the same trend with a reduction of about 75% for the vertical surfaces and up to 85% for the top surface. This shows that the cutting conditions gave better results for surfacing than contouring operations. In terms of repeatability, it is decreased for contouring, while it was improved for surfacing. This can be due to the resolution of the axes (better in the case of the Z-axis than for X and Y) as well as the stiffness of the axes (the Z-axis is actuated by a screw and nut mechanism, while X and Y axes are actuated using belts). The Z-axis of the machine is then more accurate as well as stiffer.

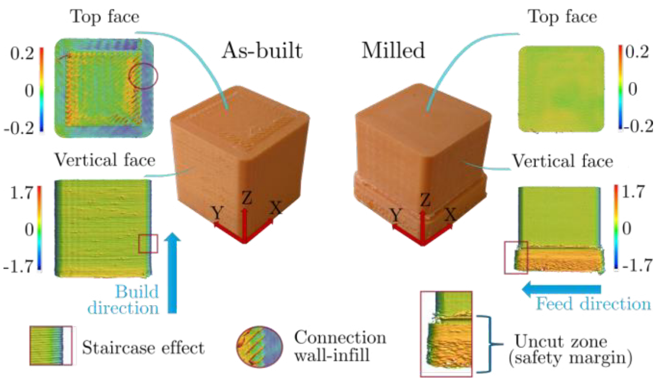

Figure 6 Qualitative analysis of the parts.

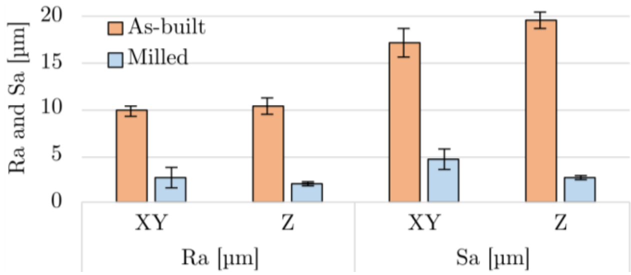

Figure 7 Arithmetic Roughness (Ra in µm) and Mean Height (Sa in µm).

The Total Roughness (Rt) and Maximum Height (Sz) followed the same overall trend, as depicted in Figure 8. Rt and Sz are decreased by about 40% on the vertical surfaces (from almost 47 µm to 28 µm for Rt and from almost 303 µm to 179 µm for Sz) and by up to 85% on the top surface (from almost 55 µm to 20 µm for Rt and from almost 750 µm to 100 µm for Sz). Again, repeatability is better when it comes to surfacing compared to the contouring operation. As it was highlighted in the qualitative evaluation of the surfaces, the top surface exhibited larger disparities before milling, explaining the larger value of Sz. The obtained surface topographies should be compared to the application foreseen for the parts. Even with the significant improvement brought by milling, the suitability of the surface topographies for the final function of the parts is still to be assessed.

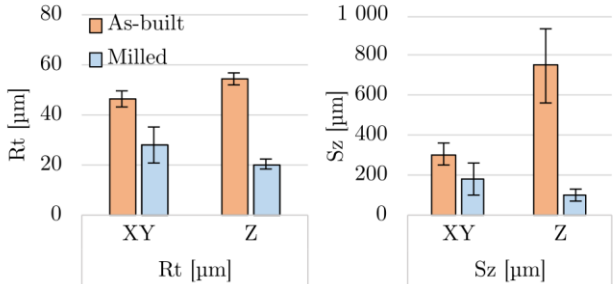

Figure 8 Total Roughness (Rt in µm) and Maximum Height (Sz in µm).

3.3. Dimensional characterization

The relative deviations to the desired dimensions of the parts (a cube with 20 mm edges) are given in Figure 9. The as-built parts exceeded the desired dimensions by about 0.190 mm on average, both for the vertical and the top surfaces. With respect to ISO 286-1:2010, this led to IT between 12 and 14, typical for FFF process conducted with the selected feedstock and printing parameters [17].

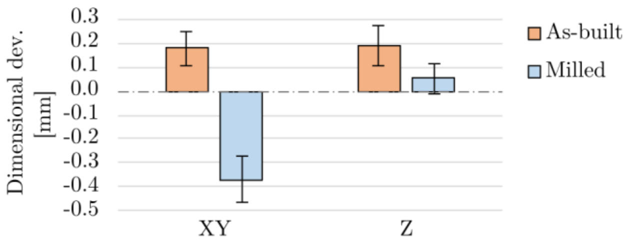

Figure 9 Dimensional deviations (in mm).

While the milling operations should improve these dimensions, it did not entirely. Indeed, the top surface almost reached the nominal dimensions with, after milling, dimensional deviations of 0.051 mm on average for the three parts. Nevertheless, large standard deviations were obtained (0.059 mm) and led to IT between 5 for the best part to 13 for the worst. Repeatability was therefore not met.

The dimensional deviations and lack of repeatability are even higher between the vertical surfaces. Values of dimensional deviations about -0.368 mm on average were obtained (IT15 and IT16) with, again, large standard deviations (0.095 mm). The origin of these very large dimensional deviations has still to be determined but it could originate from a lack of stiffness of the machine. Again, the use of belts to actuate the X and Y axes could explain the different behavior obtained for these two axes compared to the Z-axis (actuated by a screw and nut mechanism, stiffer than linear guides with belts). Making the X and Y axes stiffer is one of the major points of improvement that the machine should meet to be fully operational and deliver parts with tighter tolerances. Another perspective could be to model the machine and try to compensate for the deviations generated by its lack of stiffness.

3.4. Geometrical characterization

The geometrical deviations were significantly improved by the milling operation as shown in Figure 10.

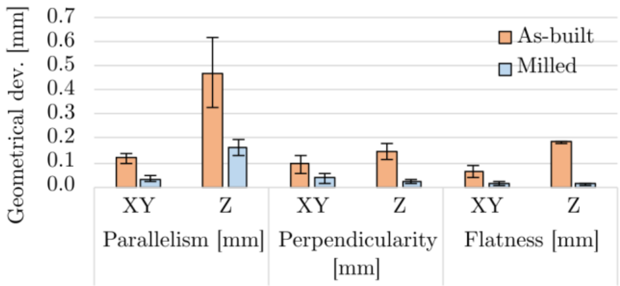

Figure 10 Geometrical deviations (in mm).

The parallelism deviation decreased by 75% and 66% for the vertical and top surfaces, respectively. This allowed the parts to reach 0.030 mm of deviation for the vertical surface and 0.160 mm for the top surface. These values belong to the H (fine) and L (large) classes of ISO 2768-2:1989. The higher deviation achieved by the top surface can be due to a lack of parallelism between the building platform and the plane containing the X and Y axes, or also to a lack of stiffness in the linear guides that hold the spindle. Furthermore, the parts were measured after their separation from the build platform. This last operation can lead to permanent deformations due to internal stresses relaxation. Nevertheless, the repeatability of both surfaces was significantly improved.

In terms of perpendicularity, the parts exhibited already low deviations in their as-built state with values below 0.100 mm for the vertical surfaces and below 0.150 mm for the top surface. These results, already satisfying an H (fine) class of ISO 2768-2:1989, were improved by milling with, again, a significant decrease of 60% and 90% for the vertical and top surfaces. The milled parts showed repeatable values of deviation between 0.020 mm and 0.036 mm.

The finish milling operation also allowed the flatness to be significantly improved from 0.065 mm to 0.013 mm (80% reduction) and from 0.185 mm to 0.010 mm (95% reduction) for the vertical and top surfaces respectively. It should be noted that, as for the perpendicularity, the as-built flatness already achieved a K (medium) class of ISO 2768-2:1989 for the vertical and top surfaces. The milling operation allowed the surface to be further improved, and it exhibited a H (fine) class of ISO 2768-2:1989 after milling.

3.5. Discussion about the stiffness of the machine

As presented in the previous sections, a lack of stiffness for the X and Y axes compared to the Z-axis can explain the differences obtained in terms of surface topographies and tolerances. This could originate from the selected type of actuation: belts for the machine X and Y axes and screw and nut mechanism for Z-axis. The X and Y belts allow speeds up to 600 mm/s to be reached according to E3D. Nevertheless, this comes at the expense of a lower stiffness and, potentially, a lack of accuracy when operating under forces. Indeed, the

E3D ToolChanger is initially devoted to 3D printing and not to milling operations. Therefore, it is not intended to hold the position of its tooltip under external forces, such as those generated during cutting operations.

During the experiments, the cutting forces could not be measured. It would have required a major modification of the build platform to insulate a dynamometer from the heated bed. A previous work [16] gives an order of magnitude for the total cutting force ($F_{tot} = \sqrt{(F_x^2 + F_y^2 + F_z^2)}$) that could be expected when milling PLA parts obtained by FFF. This could reach almost 35 N. Even if the cutting tool and parameters are not strictly identical, it gives a comparative point. An experimental analysis of the E3D ToolChanger deflection under comparable loads, and applied following the same directions, could be interesting to investigate in the future. This could guide machine design modifications and highlight the potential lack of stiffness.

4. Conclusions

Hybrid manufacturing of PLA parts by FFF and milling was conducted successfully on a modified E3D ToolChanger. The gain in terms of surface topography as well as dimensional and geometrical tolerances was evaluated:

- From a qualitative point of view, the milling operations removed the staircase effect due to the FFF process. Flat and homogeneous surfaces topographies were obtained both for vertical and top surfaces.
- A significant reduction of Ra and Sa was obtained: about 75% for the vertical surfaces and up to 85% for the top surface after milling. Rt and Sz followed the same trend and decreased by about 40% on the vertical surfaces and by up to 85% on the top surface.
- Depending on the printer axes involved, the dimensional accuracy of the parts was slightly improved (from IT14 to IT11, according to Z-axis) or degraded (from IT14 to IT15, according to X and Y axes), both with low repeatability.
- The geometrical deviations were improved by milling, with a H (fine) class of ISO 2768-2:1989 for perpendicularity and flatness. Parallelism reached a L (large) class, despite a 66% reduction of deviation.
- The repeatability of surface topography and tolerances was better for the top surface compared to the vertical surfaces. This can be due to the machine differences in terms of stiffness between the X and Y axes and the Z-axis.

This study is the first step before conducting full hybrid operations on the developed machine. The perspectives include testing other feedstock using FGF instead of the FFF process and comparing different process planning strategies in terms of production time. Despite the machine lack of stiffness, the produced parts were already significantly improved with respect to their as-built state. Quantifying the potential gain that could be obtained by milling them on a stiffer machine, using the same tool and cutting conditions could be another perspective. However, the change in position when moving from one machine to another is challenging and may introduce uncertainties, while opening new questions.

Acknowledgements

The Walloon regional government and the European Union funded this research with two projects: HybridAM and HyProPAM (grant 2110084).

References

[1] Pei E, Bernard A, Gu D, Klahn C, Monzón M, Petersen M, et al., editors. Springer Handbook of Additive Manufacturing. Cham: Springer International Publishing; 2023, doi:10.1007/978-3-031-20752-5.
[2] SmarTech Analysis. Ceramics Additive Manufacturing Markets 2017-2028, an opportunity analysis and ten-year market forecast. 2018.
[3] Altıparmak SC, Yardley VA, Shi Z, Lin J. Extrusion-based additive manufacturing technologies: State of the art and future perspectives. J Manuf Process 2022;83:607–36, doi: 10.1016/j.jmapro.2022.09.032.
[4] Golhin AP, Tonello R, Frisvad JR, Grammatikos S, Strandlie A. Surface roughness of as-printed polymers: a comprehensive review. Int J Adv Manuf Technol 2023,doi: 10.1007/s00170-023-11566-z.
[5] Stavropoulos P, Foteinopoulos P, Stavridis J, Bikas H. Increasing the industrial uptake of additive manufacturing processes: A training framework. Adv Ind Manuf Eng 2023;6:100110, doi: 10.1007/s00170-023-11566-z.
[6] Kanishka K, Acherjee B. Revolutionizing manufacturing: A comprehensive overview of additive manufacturing processes, materials, developments, and challenges. J Manuf Process 2023;107:574–619, doi: 10.1016/j.jmapro.2023.10.024.
[7] Grzesik W, Ruszaj A. Hybrid Manufacturing Processes: Physical Fundamentals, Modelling and Rational Applications. Cham: Springer International Publishing; 2021, doi: 10.1007/978-3-030-77107-2.
[8] Flynn JM, Shokrani A, Newman ST, Dhokia V. Hybrid additive and subtractive machine tools - Research and industrial developments. Int J Mach Tools Manuf 2016;101:79–101, doi: 10.1016/j.ijmachtools.2015.11.007.
[9] Lauwers B, Klocke F, Klink A, Tekkaya AE, Neugebauer R, Mcintosh D. Hybrid processes in manufacturing. CIRP Annals 2014;63:561–83, doi: 10.1016/j.cirp.2014.05.003.
[10] Hafenecker J, Bartels D, Kuball C-M, Kreß M, Rothfelder R, Schmidt M, et al. Hybrid process chains combining metal additive manufacturing and forming – A review. CIRP J Manuf Sci Technol 2023;46:98–115, doi: 10.1016/j.cirpj.2023.08.002.
[11] Guerra MG, Morfini L, Pellegrini A, Meng F, Lavecchia F, Ferraris E, et al. Material Extrusion-Debinding-Sintering as an Emerging Additive Manufacturing Process Chain for Metal/Ceramic Parts Construction. In: Tolio T, editor. CIRP Novel Topics in Production Engineering, Cham: Springer Nature Switzerland; 2024; 1:147–82, doi: 10.1007/978-3-031-54034-9_5.
[12] Tejada Martinez LV, Witz J-F, Najjar D, Boidin X, Lesaffre F, Martin V, et al. Hybrid FFF/CNC: An open source hardware & software system. HardwareX 2024;18:e00536, doi: 10.1016/j.ohx.2024.e00536.
[13] Dilberoglu UM, Gharehpapagh B, Yaman U, Dolen M. Current trends and research opportunities in hybrid additive manufacturing. Int J Adv Manuf Technol 2021;113:623–48, doi: 10.1007/s00170-021-06688-1.
[14] Dilberoglu UM, Yaman U, Dolen M. A comprehensive guide to milling techniques for smoothing the surfaces of 3D-printed thermoplastic parts. Rapid Prototyp J 2024;30:1648–62, doi: 10.1108/RPJ-08-2023-0277.
[15] Pei E, Rosen DW, Seepersad C. Design Rules. In: Seifi M, Bourell DL, Frazier W, Kuhn H, editors. Additive Manufacturing Design and Applications, ASM International; 2023, p. 97–115, doi: 10.31399/asm.hb.v24A.a0006948.
[16] Lorenzoni M, Spitaels L, Rivière-Lorphèvre E, Odent J, M'Saoubi R, Cloëz L, et al. Investigation on cutting fluid use in finish milling of polylactide (PLA) 3D-printed parts. Procedia CIRP 2025;133:656–61, doi: 10.1016/j.procir.2025.02.112.
[17] Spitaels L, Nieto Fuentes E, Rivière-Lorphèvre E, Arrazola P-J, Ducobu F. A Systematic Method for Assessing the Machine Performance of Material Extrusion Printers. J. Manuf. Mater. Process. 2024;8:36, doi: 10.3390/jmmp8010036.